

High-power ultrafast thin disk laser oscillators and their potential for sub-100-femtosecond pulse generation

T. Südmeyer · C. Kränkel · C.R.E. Baer · O.H. Heckl ·
C.J. Saraceno · M. Golling · R. Peters · K. Petermann ·
G. Huber · U. Keller

Received: 17 April 2009 / Revised version: 26 June 2009 / Published online: 15 September 2009
© The Author(s) 2009. This article is published with open access at Springerlink.com

Abstract Ultrafast thin disk laser oscillators achieve the highest average output powers and pulse energies of any mode-locked laser oscillator technology. The thin disk concept avoids thermal problems occurring in conventional high-power rod or slab lasers and enables high-power TEM₀₀ operation with broadband gain materials. Stable and self-starting passive pulse formation is achieved with semiconductor saturable absorber mirrors (SESAMs). The key components of ultrafast thin disk lasers, such as gain material, SESAM, and dispersive cavity mirrors, are all used in reflection. This is an advantage for the generation of ultrashort pulses with excellent temporal, spectral, and spatial properties because the pulses are not affected by large nonlinearities in the oscillator. Output powers close to 100 W and pulse energies above 10 μ J are directly obtained without any additional amplification, which makes these lasers interesting for a growing number of industrial and scientific applications such as material processing or driving experiments in high-field science. Ultrafast thin disk lasers are based on a power-scalable concept, and substantially higher power levels appear feasible. However, both the highest power levels and pulse energies are currently only achieved with Yb:YAG as the gain material, which limits the gain bandwidth and therefore the achievable pulse duration to 700 to 800 fs in

efficient thin disk operation. Other Yb-doped gain materials exhibit a larger gain bandwidth and support shorter pulse durations. It is important to evaluate their suitability for power scaling in the thin disk laser geometry. In this paper, we review the development of ultrafast thin disk lasers with shorter pulse durations. We discuss the requirements on the gain materials and compare different Yb-doped host materials. The recently developed sesquioxide materials are particularly promising as they enabled the highest optical-to-optical efficiency (43%) and shortest pulse duration (227 fs) ever achieved with a mode-locked thin disk laser.

PACS 42.55.Rz · 42.55.Xi · 42.60.Fc · 42.65.Re · 42.70.Hj

1 Introduction

Since its first demonstration in the year 2000 [1], the SESAM mode-locked thin disk laser technology achieved higher pulse energies and average power levels than any other mode-locked laser oscillator [2, 3]. The first mode-locked thin disk laser was based on the Yb:YAG gain material and allowed to increase the average power of femtosecond oscillators from previously below 4 to 16 W. The key advantage of the SESAM-mode-locked thin disk laser is its power scalability. The output power can be scaled up by increasing the pump power and mode areas on both gain medium and SESAM by the same factor. Successful power scaling resulted in 80 W average output power [4, 5], which was obtained with an approximately five times larger pump area than in the first mode-locked thin disk laser. The pulse energy of ultrafast thin disk lasers was also successfully increased. Pulse energies as high as 11.3 μ J [6] were generated in a cavity geometry with the thin disk used as simple folding mirror, while up to 25.9 μ J were achieved in an active

T. Südmeyer (✉) · C. Kränkel · C.R.E. Baer · O.H. Heckl ·
C.J. Saraceno · M. Golling · U. Keller
Physics Department, Institute of Quantum Electronics,
ETH Zurich, Wolfgang-Pauli Strasse 16, 8093 Zurich,
Switzerland
e-mail: sudmeyer@phys.ethz.ch
Fax: +41-44-6331059

R. Peters · K. Petermann · G. Huber
Institute of Laser-Physics, University of Hamburg, Luruper
Chaussee 149, 22761 Hamburg, Germany

multipass cavity with 13 reflections on the disk [7]. Generating energetic femtosecond pulses directly from a laser oscillator without any further amplification has a number of advantages in terms of simplicity, compactness, and low-noise operation [3]. Based on the previous results, we believe that the ultrafast thin disk laser technology will support further scaling towards several hundred watts of average output power and pulse energies exceeding 100 μJ [3]. So far all these results proving the power scaling possibilities of the thin disk laser concept have been achieved with the gain material Yb:YAG, which is nowadays the best developed thin disk gain material. High-quality disks are available from different manufacturers, because several companies use Yb:YAG thin disks in multikilowatt continuous-wave (CW) laser products. The initial choice of Yb:YAG was not influenced by its suitability to support the generation of femtosecond pulses. It was selected because of its easy growth, high gain cross section compared to other Yb-doped laser materials, relaxed demands on the pump diodes and thermomechanical strength to sustain high power levels. The limited gain bandwidth of Yb:YAG does not support pulse durations shorter than approximately 700 fs in efficient high-power thin disk operation [8] even if pulses as short as 340 fs have been achieved in low-power SESAM-mode-locked laser oscillators [9]. Longer pulse durations can easily be achieved by inserting a spectral filter into the thin disk laser cavity [8]. Using a 60- μm -thick etalon, the pulse duration of an Yb:YAG thin disk laser was continuously tuned over a wide range—from 3.3 to 89 ps—simply by changing the intracavity dispersion [10]. Pulses with a few picoseconds duration are ideally suited for many industrial laser micromachining applications. However, other application fields rely on substantially shorter pulse durations. An important example is that of high-field science experiments, which previously required complex amplifier systems operating at low repetition rates of the order of kilohertz. In contrast, ultrafast thin disk lasers operate at megahertz repetition rates and allow for substantially shorter measurement times and an improved signal-to-noise ratio [3]. A promising area for ultrafast thin disk lasers is high-harmonic generation [11, 12] at high power levels. The resulting table-top megahertz VUV/XUV sources with high photon flux would have a strong impact in fields as diverse as medicine, biology, chemistry, physics, and material science. Currently, high-field experiments with Yb:YAG thin disk lasers require external pulse compression [13, 14]. Reducing the pulse duration by employing new thin disk gain materials with larger bandwidths is a promising alternative towards lower complexity of the laser system and therefore more compact table-top sources.

Several other laser materials exhibit a larger gain bandwidth than Yb:YAG. Ti:Sapphire material currently holds the record for the shortest generated pulses in mode-locked

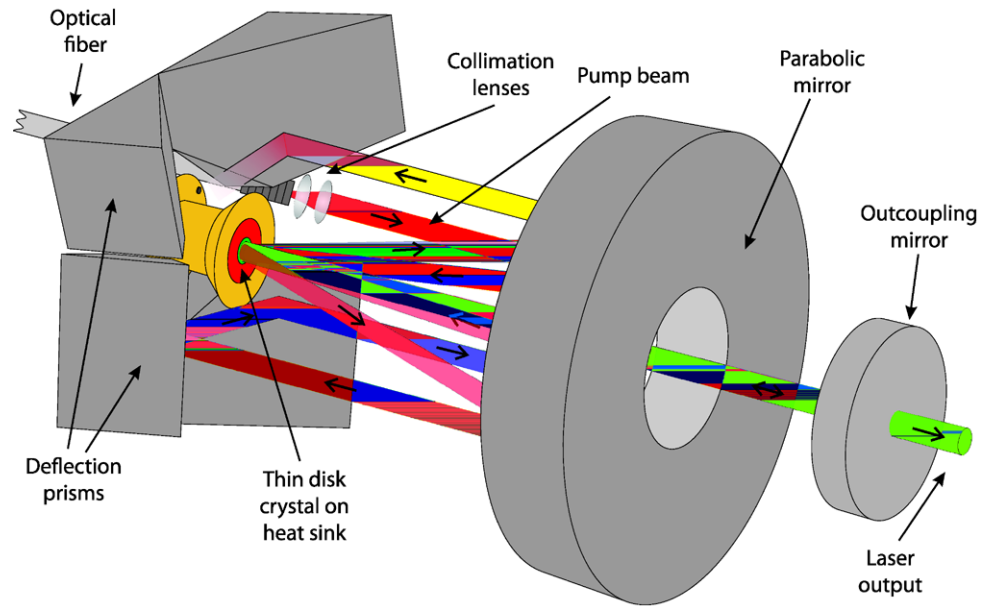
operation with sub-6-fs pulse duration. Unfortunately, it is not suitable for power scaling to highest power levels because of thermal issues (see Sect. 4). Furthermore, it requires a pump wavelength in the blue-green spectral region, for which no high-power diodes are available. Among the directly diode pumpable gain materials, Yb-doped materials are particularly promising [9, 15, 16]. So far there have been more than ten Yb-doped host materials that generated sub-100-fs pulses in a standard bulk gain medium mode-locked laser oscillator design (see Table 2). Average output power levels of up to 1.5 W were obtained [17]. Unfortunately, it is usually not possible to directly transfer these results to an efficient high-power mode-locked ultrafast thin disk laser. In fact, a suitable gain material for thin disk operation has to fulfill several requirements, not only with respect to its laser properties, but also in terms of thermomechanical strength and other material properties. Furthermore, the technical aspects are challenging: high-quality gain materials have to be manufactured in sufficiently large size, polished to thin disks of 50–300 μm thickness and at least several millimeters diameter, coated, and stress-free mounted onto a heat sink. Due to these challenges only two thin disk gain materials had been mode-locked by the year 2007: Yb:YAG and Yb:KYW [18]. Recently, there has been a large research effort to establish novel thin disk gain materials, which combine the excellent power scaling properties of Yb:YAG with a larger emission bandwidth. Novel thin disk gain materials such as Yb:Lu₂O₃ or Yb:LuScO₃ were introduced [19, 20], which resulted in higher optical-to-optical efficiencies and shorter pulse durations than previous ultrafast thin disk lasers [21, 22].

In this paper, we will review gain materials for efficient high-power femtosecond thin disk laser operation. We discuss the demands on these gain materials in terms of laser and thermomechanical properties, and the trade-offs in pulse duration with higher power. We then present an overview of different Yb-doped materials and compare their suitability for the thin disk approach. Finally, we give an outlook towards other new gain materials.

2 Mode-locked thin disk lasers

The development of high-power ultrafast lasers depends strongly on the availability of high-power CW lasers with fundamental transverse mode operation (i.e., TEM₀₀ mode). The presence of multiple higher order transverse modes with different frequency spacing leads to mode competition and mode locking instabilities. Achieving fundamental transverse mode operation is particularly challenging for high average powers because of the high thermal load on the intracavity optical components. This is particularly true for the gain medium, in which a substantial amount of heat

Fig. 1 Schematic setup of the thin disk pump configuration with the disk in the focal plane of a parabolic mirror. The pump optics is usually aligned for 16 or 24 passes through the gain medium



is generated by the pump radiation due to the quantum defect between the pump and laser wavelength and other additional parasitic processes. The resulting thermal gradients can introduce wave front distortions leading to thermal lensing and/or aberrations, which can strongly degrade the transverse beam quality. These problems are usually particularly severe for gain materials with a large emission bandwidth necessary for femtosecond pulse generation. Many of these materials have a disordered crystal structure, and the broad emission spectrum takes its origin in different lattice environments for the laser active ions [23]. However, this disordered lattice restricts the propagation of phonons, which often leads to a significantly lowered thermal conductivity.

During the last decade, two laser geometries have proven to support the highest power levels in fundamental transverse mode operation: thin disk lasers and fiber lasers. Both geometries have excellent heat transport capabilities, because the ratio between cooling surface and active volume is large. Using fiber lasers CW power levels above 1 kW were demonstrated with nearly diffraction-limited transverse mode quality [24]. Nevertheless, they are not ideal candidates for mode-locked femtosecond high-power operation because the large amount of nonlinear effects limits stable pulse formation. Therefore, high-power levels are only achieved with complex amplifier systems [25–27].

The other geometry is the thin disk laser [28], which so far has supported 360 W CW output power in a fundamental transverse mode [29, 30] and 5.3 kW at 65% optical-to-optical efficiency in multimode operation [29]. As the name implies, in this geometry, the gain material is shaped into a very thin disk. Its typical thickness of 50 to 300 μm is small compared to the diameters of the pumped area and the laser beam which are usually a few millimeters. The disk

has a highly reflective coating on one side and an antireflective coating on the other side for both, pump and laser wavelength. The reflective side is mounted directly onto a water-cooled heat sink and the disk is used in reflection. The thin disk therefore acts as an active mirror. It can be cooled very efficiently and the heat flow is mainly one-dimensional towards the heat sink, i.e., collinear to the direction of the laser beam. The thermal gradients in the transverse direction are weak, and thermal lensing is therefore strongly reduced compared to a rod or slab design. The pump absorption in a single pass through the thin disk is low but highly efficient operation is achieved by arranging multiple pump passes through the disk (typically 16 or 24 passes), see Fig. 1.

Stable femtosecond pulse formation is achieved using a semiconductor saturable absorber mirror (SESAM [31, 32]), which acts as a nonlinear loss modulator. Such a device exhibits higher reflectivity for higher pulse fluences and therefore favors pulsed over CW operation. The key advantage of the SESAM is its large flexibility to optimize the absorber parameters [33, 34], which prevents mode locking instabilities such as Q-switched mode locking [35]. SESAM designs for high-power thin disk lasers often use a dielectric top coating for the reduction of two-photon absorption (Fig. 2) [6] and an increased damage threshold. The precise measurement of the nonlinear absorption coefficients are discussed in [36, 37].

Ultrafast thin disk lasers usually rely on soliton mode locking [38–40], for which the SESAM only needs to start and stabilize the mode locking process. The final pulse formation is controlled by soliton pulse shaping which balances the negative total intracavity group delay dispersion (GDD) with self-phase modulation (SPM) [15]. Soliton mode locking has the advantage that it relaxes the requirements on the

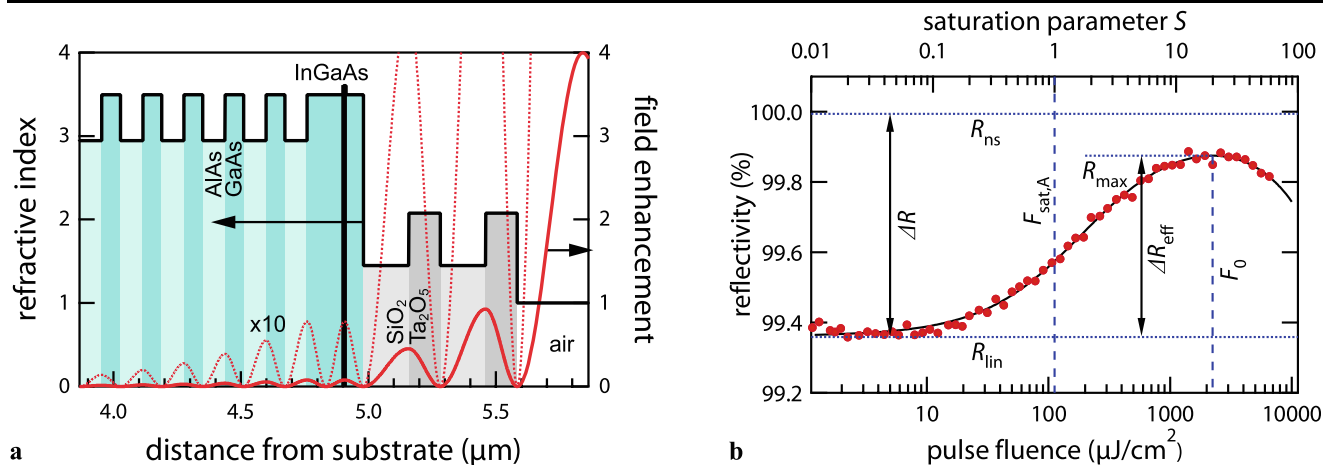


Fig. 2 (a) Refractive index pattern and field enhancement of an antiresonant SESAM with a top mirror consisting of two $\text{SiO}_2/\text{Ta}_2\text{O}_5$ -Bragg pairs. The dotted curve is the field enhancement multiplied by a factor of ten. (b) Reflectivity measurement (dots) as a function of the incident pulse fluence for a SESAM with dielec-

tric top coating. The fit (solid line) results in a saturation fluence of $F_{A,\text{sat}} = 112 \mu\text{J}/\text{cm}^2$, a modulation depth of $\Delta R = 0.64\%$ and non-saturable losses of $\Delta R_{\text{ns}} < 0.01\%$. The measurement was done with 570-fs pulses at 1034 nm

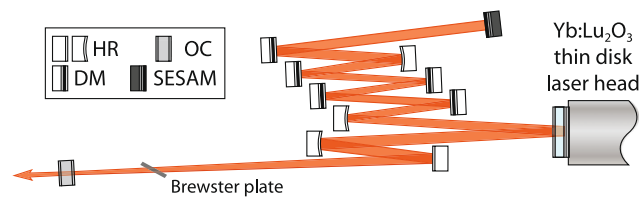


Fig. 3 Schematic of the $\text{Yb}:\text{Lu}_2\text{O}_3$ thin disk laser cavity (not to scale). HR: highly reflective mirror, DM: dispersive mirror, OC: output coupler, SESAM: semiconductor saturable absorber mirror

recovery time of the SESAM [41], reduces Q-switching instabilities [35], and generates transform-limited clean soliton pulses even at the highest pulse energies [6]. Chirped-pulse operation in the positive dispersion regime, which is an interesting technique for operating at reduced intra-cavity intensity levels, has also been investigated with an $\text{Yb}:\text{KLuW}$ thin disk laser [42]. However, external pulse compression is required and the generated pulses are not ideal transform-limited solitons.

A typical cavity design is shown in Fig. 3 for the $\text{Yb}:\text{Lu}_2\text{O}_3$ thin disk laser discussed in Ref. [21]. The laser setup uses a 250- μm -thick $\text{Yb}:\text{Lu}_2\text{O}_3$ disk, which is used as a folding mirror inside a standing-wave cavity. The disk is pumped by a fiber-coupled diode laser. The pump module is arranged for 24 passes through the gain medium and a pump spot diameter of 1.2 mm. For passive mode locking, a SESAM is used as an end mirror. The nonlinear reflectivity curve of a typical SESAM is shown in Fig. 2. A fused silica Brewster plate is inserted to provide the SPM required for stable soliton pulses and to ensure linear polarization of the laser beam. The outcoupling transmission is 5.2% at the laser wavelength of 1034 nm.

Compared to other solid-state laser designs, the thin disk laser has the least amount of material inside the optical resonator, because all the key components of the passively mode-locked thin disk laser are used in reflection. This is a major advantage for the generation of femtosecond pulses with excellent temporal, spectral, and spatial properties, because the pulses are not affected by excessive Kerr non-linearity inside the resonator. The concept of the SESAM-mode-locked thin disk laser has the crucial advantage of power scalability. The output power can be scaled up by multiplying the pump power and the mode areas on both gain medium and SESAM by the same factor. The temperature of the thin disk will not rise if the cooling system is capable of removing the additional heat. This scaling procedure avoids damage on the key components because the intensities on the disk and on the absorber remain unchanged. Another important point is that the saturation of the gain and the SESAM remains constant, which is important for preventing mode locking instabilities [8].

3 Disk requirements

It is a challenging task to establish a suitable thin disk gain material for femtosecond pulse generation at several tens of watts of average power. The key requirement is a sufficiently large emission bandwidth, which supports the generation of femtosecond pulses. Another important property is the availability of suitable high-power pump sources. The gain material should exhibit an absorption spectrum accessible to direct pumping by high-power laser diodes. Such diodes are nowadays commercially available at 808, 880, 915, 940,

and 980 nm. The emission bandwidth of the high-power diodes has to match the absorption bandwidth of the material, which might require a stringent selection of the individual diode bars (typically $\Delta\lambda_{\text{diode}} < 3\text{--}5$ nm) or additional wavelength stabilization, e.g., with a volume Bragg grating (VBG) (typically $\Delta\lambda_{\text{diode}} < 0.5$ nm) [43, 44]. For optimized thermal management in the laser crystal the gain material should exhibit a small quantum defect, i.e., a laser wavelength close to the pump wavelength. Furthermore, other parasitic heat generating processes should be minimized. Efficient high-power thin disk lasers are usually operated at comparably high inversion levels and it is challenging to suppress parasitic processes, such as nonradiative relaxations, excited state absorption, or up-conversion processes. For low laser threshold and high optical-to-optical efficiency the emission cross section and the fluorescence lifetime have to be large. A high emission cross section is also beneficial to overcome Q-switched mode locking instabilities [35].

It is an advantage of the thin disk laser concept that even materials with a relatively poor thermal conductivity can be used at high power levels [29]. However, to reduce thermal lensing and aberrations, a high thermal conductivity and low temperature dependence of the refractive index is advantageous. Furthermore, the thin disk geometry requires suitable thermomechanical properties of the host material. A good mechanical strength is crucial, not only for laser operation but also for the preparation of thin disks with large diameters. Despite the efficient heat transport in the thin disk approach, strong thermal gradients occur at laser operation, which increase the tendency for thermally induced stress fracture. Furthermore, the absorption of the thin disk has to be large enough to efficiently use the available pump power after the typical 16 or 24 passes through the disk. Besides improving the laser efficiency, a large absorption also helps to prevent damage by the nonabsorbed pump radiation. In the usual pump geometry, the nonabsorbed radiation is reflected backwards and can cause damage of the pump diodes, respectively the fiber output surface of fiber-coupled diodes. If the pump absorption coefficient is low, the required thickness of the disk becomes larger, and the maximum crystal temperature increases. This results in thermal lensing and aberrations, which can prevent TEM₀₀ operation and can even lead to damage. Moreover, high temperature compromises the efficiency for three-level laser materials. For a high absorption coefficient a large absorption cross section and a high doping density is required.

In summary, a suitable material should exhibit the following properties:

1. Sufficiently large emission bandwidth $\Delta\lambda_{\text{laser}}$ supporting the generation of femtosecond pulses
2. Pump absorption wavelength λ_{pump} and bandwidth $\Delta\lambda_{\text{pump}}$ matched by available high-power pump lasers

3. Small quantum defect $(1 - \lambda_{\text{pump}}/\lambda_{\text{laser}})$ to minimize heat load
4. Absence of parasitic processes such as nonradiative relaxations, excited state absorption, up-conversion, and cross-relaxation
5. High emission cross section and high fluorescence lifetime to minimize the laser threshold
6. High pump absorption cross sections and high doping concentrations to minimize the disk thickness
7. High thermal conductivity for efficient heat removal
8. Low temperature dependence of the refractive index for low thermal lensing
9. High mechanical strength and weak tendency towards thermally induced stress fracture

4 Gain materials and achieved mode locking results

In Tables 1, 2, we list the properties of a certain number of attractive gain materials with large bandwidths, and some mode locking results that have been achieved. A more detailed list of mode-locked results obtained for various other gain materials is presented in [15]. It is important to emphasize that experiments at low average output power only prove the suitability of a gain material to generate short femtosecond pulses. Unfortunately, one cannot expect to easily transfer such a performance to efficient operation with tens of watts output power. The materials have to fulfill the requirements previously discussed, otherwise the output power will be restricted to a few watts despite the excellent heat transport capabilities of the thin disk geometry.

4.1 Expected pulse duration in the thin disk configuration

Table 2 shows that the pulse durations obtained in low power lasers are usually shorter than in high-power configurations. The minimum achievable pulse duration τ_p for stable soliton mode locking with a SESAM is in detail investigated in [38, 41]. The main limitations are determined by the saturated gain g and the gain bandwidth Δf_g according to

$$\tau_p \propto \frac{g^{3/8}}{(\Delta f_g)^{3/4}}.$$

Compared to low power oscillators, high-power thin disk lasers usually use a large degree of output coupling and operate at a higher saturated gain. Increasing g from 1 to 10% increases the minimum achievable pulse duration by more than a factor of two (if other parameters such as recovery time of the SESAM, its modulation depth, and the maximum acceptable nonlinear phase change of the circulating pulse per roundtrip remain constant, for a detailed discussion see Ref. [41]). Furthermore, the large saturated gain must be achieved from a thin gain medium. This requires

Table 1 Overview of different gain materials for ultrashort pulse generation. The given absorption cross sections for anisotropic materials correspond to the average over all polarizations, which is usually a good approximation in the thin disk pump geometry. To estimate the minimum achievable pulse duration, it is usually not sufficient to consider a FWHM bandwidth of the gain spectrum. Instead, the inversion-dependent shape has to be taken into account (see Fig. 4). Abbreviations: HEM = heat exchanger method, Cz = Czochralski growth, Flux = flux method

| Properties | Symbol/Unit | Ti:Sapphire Ti:Al ₂ O ₃ | Yb:YAG Yb:Y ₃ Al ₅ O ₁₂ | Yb:YAB Yb:YAl ₃ (BO ₃) ₄ | Yb:CAIGO Yb:CaGdAlO ₄ |
|---|---|--|---|---|-------------------------------------|
| Laser properties | | | | | |
| pump wavelength | λ_P/nm | typ. 488 or 532 | 940 | 975 | 979 |
| absorption bandwidth (FWHM) | $\Delta\lambda_P/\text{nm}$ | > 100 nm | 12.5 | 20 | > 5 |
| quantum defect | % | 67 | 91 | 93 | 96 |
| absorption cross section at λ_P (average) | $\sigma_{\text{abs},P}/(10^{-20}\text{cm}^2)$ | 6 | 0.83 | 2.8 | 1.56 |
| emission cross section at λ_L | $\sigma_{\text{em},L}/(10^{-20}\text{cm}^2)$ | 41 | 1.89 | 0.35 | 0.75 |
| fluorescence lifetime | $\tau_{\text{rad}}/\mu\text{s}$ | 3.2 | 940 | 450 | 420 |
| Other material properties | | | | | |
| thermal conductivity (average) | $K/(\text{W}/(\text{m K}))$ | 33 | ~11 | 4.7 | 6.6 |
| hardness | Mohs | 9 | 8.5 | 7.5 | – |
| max. at.% for lasing ^a | at.% | 0.25 | 12 | 30 | 13 |
| cation density | $10^{22}/\text{cm}^3$ | 4.7 | 1.38 | 0.55 | 1.25 |
| max. absorption for lasing | $\alpha_{\text{abs}}/\text{cm}^{-1}$ | 7.0 | 13.7 | 46.2 | 25.3 |
| dn/dT | $(dn/dT)/(10^{-6}/\text{K})$ | 13 | 9.9 | 11 | – |
| Symmetry | | hexagonal uniaxial | cubic isotropic | trigonal uniaxial | tetragonal uniaxial |
| Growth | | Cz | Cz | Flux | Cz |
| Reference | | [81–83] | [84, 85] | [86, 87] | [88] |
| Laser properties | | | | | |
| pump wavelength | λ_P/nm | 976 | 975 | 977 | 975.6 |
| absorption bandwidth (FWHM) | $\Delta\lambda_P/\text{nm}$ | 2.9 | 2.1 | 2.1 | 2.4 |
| quantum defect | % | 94 | 94 | 95 | 94 |
| absorption cross section at λ_P (average) | $\sigma_{\text{abs},P}/(10^{-20}\text{cm}^2)$ | 3.06 | 4.44 | 2.4 | 3.3 |
| emission cross section at λ_L | $\sigma_{\text{em},L}/(10^{-20}\text{cm}^2)$ | 1.26 | 1.44 | 0.92 | 0.89 |
| fluorescence lifetime | $\tau_{\text{rad}}/\mu\text{s}$ | 870 | 850 | 850 | 850 |
| Other material properties | | | | | |
| thermal conductivity (average) | $K/(\text{W}/(\text{m K}))$ | 12.8 | 18 | 13.4 | 3.9 |
| hardness | Mohs | 6–6.5 | 6.5 | 6.5 | 6.5 |
| max. at.% for lasing | at.% | 5 | 5 | 5 | 5 |
| cation density | $10^{22}/\text{cm}^3$ | 2.85 | 3.36 | 2.69 | 3.1 |
| max. absorption for lasing | $\alpha_{\text{abs}}/\text{cm}^{-1}$ | 43.6 | 74.6 | 32.6 | 51.2 |
| dn/dT | $(dn/dT)/(10^{-6}/\text{K})$ | 8.6 | 9.6 | 8.5 | ~9 |
| Symmetry | | cubic isotropic | cubic isotropic | cubic isotropic | cubic isotropic |
| Growth | | HEM | HEM | HEM | HEM |
| Reference | | | | [67] | |

Table 1 (Continued)

| Properties | Symbol/Unit | Yb:KGW Yb:KGd(WO ₄) ₂ | Yb:KYW Yb:KY(WO ₄) ₂ | Yb:KLuW Yb:KLu(WO ₄) ₂ | Yb:NGW Yb:NaGd(WO ₄) ₂ |
|---|---|---|--|--|--|
| Laser properties | | | | | |
| pump wavelength | λ_P/nm | 981 | 981 | 981 | 975 |
| absorption bandwidth (FWHM) | $\Delta\lambda_P/\text{nm}$ | 3.7 | 3.5 | 3.6 | 8 |
| quantum defect | % | 94 | 94 | 94 | 95 |
| absorption cross section at λ_P (average) | $\sigma_{\text{abs},P}/(10^{-20} \text{ cm}^2)$ | 5.3 | 6.3 | 4.4 | 1.5 |
| emission cross section at λ_L | $\sigma_{\text{em},L}/(10^{-20} \text{ cm}^2)$ | 2.8 (a) | 3 (a) | 2.5 | ~0.1 |
| fluorescence lifetime | $\tau_{\text{rad}}/\mu\text{s}$ | 243 | 233 | 254 | 370 |
| Other material properties | | | | | |
| thermal conductivity (average) | $K/(W/(m \text{ K}))$ | ~3.3 | – | ~3.3 | ~1.2 |
| hardness | Mohs | 4–5 | 4–5 | – | 4.5 |
| max. at.% for lasing | at.% | 25 | 25 | 25 | 25 |
| cation density | $10^{22}/\text{cm}^3$ | 0.64 | 0.63 | 0.63 | 0.64 |
| max. absorption for lasing | $\alpha_{\text{abs}}/\text{cm}^{-1}$ | 84.8 | 94.5 | 69.3 | 24 |
| dn/dT | $(dn/dT)/(10^{-6}/\text{K})$ | ^b | ^b | ^b | 107/42 |
| Symmetry | | monoclinic biaxial | monoclinic biaxial | monoclinic biaxial | tetragonal uniaxial |
| Growth | | Flux | Flux | Flux | Cz |
| Reference | | | [89] | [72] | [67] |
| Laser properties | | | | | |
| pump wavelength | λ_P/nm | 985 | 985 | 976 | 981 |
| absorption bandwidth (FWHM) | $\Delta\lambda_P/\text{nm}$ | 7.9 | 5.8 | 2.3 | >30 |
| quantum defect | % | 96 | 96 | 94 | 94 |
| absorption cross section at λ_P (average) | $\sigma_{\text{abs},P}/(10^{-20} \text{ cm}^2)$ | 3.3 | 4 | 1.05 | 0.51 |
| emission cross section at λ_L | $\sigma_{\text{em},L}/(10^{-20} \text{ cm}^2)$ | 0.7 | 0.5 | 0.45 | 0.25 |
| fluorescence lifetime | $\tau_{\text{rad}}/\mu\text{s}$ | 310 | 300 | 2200 | 1150 |
| Other material properties | | | | | |
| thermal conductivity (average) | $K/(W/(m \text{ K}))$ | ~7 | ~8 | ~2 | 2.8 |
| hardness | Mohs | 5 | 6 | 6–6.5 | 6 |
| max. at.% for lasing | at.% | 2 | 2 | 35 | 25 |
| cation density | $10^{22}/\text{cm}^3$ | 1.26 | 1.31 | 0.45 | 0.45 |
| max. absorption for lasing | $\alpha_{\text{abs}}/\text{cm}^{-1}$ | 8.3 | 10.5 | 16.5 | 5.7 |
| dn/dT | $(dn/dT)/(10^{-6}/\text{K})$ | 8.5/3.9 | – | 0.62/0.8/0.17 | 4.4 |
| Symmetry | | tetragonal uniaxial | tetragonal uniaxial | monoclinic biaxial | quasi-trigonal uniaxial |
| Growth | | Cz | Cz | Cz | Cz |
| Reference | | | | [66] | |

^aMax at.% refers to the maximum doping concentration that can be used for efficient thin disk laser operation. In cases where no max. at.% is given by the crystal structure or in the literature, the value was calculated assuming the same ion density like in Yb:YAG at 12 at.% [90]

^bStrong variations in the reported values of the thermo-optic coefficients in the potassium tungstates ranging from positive to negative values (depending on the orientation) make it impossible to state reasonable average values

Table 2 Comparison of ultrafast lasers based on different gain materials. A more detailed overview including a discussion of the mode locking techniques is given in Ref. [15]

| Laser material | | ML technique | λ_0/nm | τ_p/fs | P_{ave}/mW | $f_{\text{rep}}/\text{MHz}$ | Ref. |
|----------------|---|--------------|-----------------------|--------------------|----------------------------|-----------------------------|--------------------|
| Ti:sapphire | $\text{Ti}^{3+}:\text{Al}_2\text{O}_3$ | KLM | ~ 800 | 54 | 3500 | 6.23 | [91] |
| | | KLM | ~ 800 | <40 | 2500 | 50 | [92] |
| | | KLM | ~ 800 | <40 | 1000 | 2 | [92] |
| | | KLM | ~ 800 | <6 | 120–300 | 65–85 | [47, 48, 93, 94] |
| Yb:glass | Yb:silicate glass | SESAM | 1045 | 61 | 65 | 112 | [50] |
| | Yb:phosphate glass | SESAM | 1050 | 58 | 65 | 112 | [50] |
| Yb:YAG | $\text{Yb}^{3+}:\text{Y}_3\text{Al}_5\text{O}_{12}$ | SESAM | 1030 | 705 | 80000 | 57 | [4] |
| | | SESAM | 1033 | 340 | 170 | ^b | [9] |
| | | KLM | 1051 | 100 | 151 | 150 | [95] |
| | | SESAM | 1030 | 2200 | 8100 | 63 | [96] |
| Yb:YAB | $\text{Yb:YAl}_3(\text{BO}_3)_4$ | SESAM | 1050 | 87 | 61 | 92 | [97] |
| Yb:CALGO | Yb:CaGdAlO_4 | SESAM | 1043 | 47 | 38 | 109 | [98] |
| | | SESAM | 1043 | 93 | 650 | 27 | [99] |
| Yb:CaF | Yb:CaF_2 | SESAM | 1049 | 230 | 1740 | ^b | [100] |
| Yb:LuO | $\text{Yb:Lu}_2\text{O}_3$ | KLM | 1032 | 65 | 320 | 99 | [64] |
| | | SESAM | 1034 | 535 | 63000 | 81 | [69, 70] |
| | | SESAM | 1035 | 329 | 40000 | 81 | [69] |
| Yb:ScO | $\text{Yb:Sc}_2\text{O}_3$ | SESAM | 1044 | 230 | 540 | 86 | [101] |
| Yb:YO | $\text{Yb:Y}_2\text{O}_3$ | KLM | 1036 | 68 | 540 | 99 | [17] |
| Yb:LuScO | Yb:LuScO_3 | SESAM | 1036 | 111 | 34 | 92 | [102] |
| | | SESAM | 1041 | 227 | 7200 | 66.5 | [22] |
| Yb:YO + Yb:ScO | | KLM | 1041 | 66 | 1500 | 89 | [17] ^a |
| Yb:KGW | $\text{Yb}^{3+}:\text{KGd}(\text{WO}_4)_2$ | SESAM | 1037 | 100 | 126 | ^b | [103] |
| | | SESAM | 1037 | 176 | 1100 | 86 | [104] |
| | | SESAM | 1039 | 290 | 9900 | 45 | [105] |
| Yb:KYW | $\text{Yb}^{3+}:\text{KY}(\text{WO}_4)_2$ | KLM | 1046 | 71 | 120 | 110 | [106] |
| | | SESAM | 1029 | 240 | 22000 | 25 | [18] |
| | | SESAM | 1043 | 470 | 17000 | 79.8 | [107] ^a |
| Yb:KLuW | $\text{Yb:KLu}(\text{WO}_4)_2$ | SESAM | 1030 | 81 | 70 | 95 | [108] |
| | | SESAM | ^b | 490 | 25600 | 34.7 | [53] |
| Yb:NGW | $\text{Yb}^{3+}:\text{NaGd}(\text{WO}_4)_2$ | SESAM | 1032 | 75 | 23 | ^b | [109] |
| Yb:NYW | $\text{Yb}^{3+}:\text{NaY}(\text{WO}_4)_2$ | SESAM | 1035 | 53 | 91 | 96 | [110] |
| Yb:YVO | Yb:YVO_4 | KLM | 1050 | 61 | 54 | 105 | [76] |
| Yb:GdVO | Yb:GdVO_4 | SESAM | 1019 | 3100 | 1010 | 135 | [111] |
| Yb:LuVO | Yb:LuVO_4 | SESAM | 1036 | 58 | 85 | 94 | [77] |
| Yb:YCOB | $\text{Yb:Ca}_4\text{YO}(\text{BO}_3)_3$ | SESAM | 1056 | 76 | 16 | 94 | [112] |
| Yb:GdCOB | $\text{Yb}^{3+}:\text{Ca}_4\text{GdO}(\text{BO}_3)_3$ | SESAM | 1045 | 90 | 40 | 100 | [113] |
| Yb:LSB | $\text{Yb:LaSc}_3(\text{BO}_3)_4$ | SESAM | 1053 | 58 | 73 | 90 | [114] |
| Yb:BOYS | $\text{Yb}^{3+}:\text{Sr}_3\text{Y}(\text{BO}_3)_3$ | SESAM | 1062 | 69 | 80 | 113 | [115] |
| Yb:YSO | $\text{Yb:Y}_2\text{SiO}_5$ | SESAM | 1044 | 198 | 2600 | 75 | [116] |
| Yb:SYS | $\text{Yb}^{3+}:\text{SrY}_4(\text{SiO}_4)_3\text{O}$ | SESAM | 1066 | 70 | 156 | 98 | [117] |
| Yb:LSO | $\text{Yb:Lu}_2\text{SiO}_5$ | SESAM | 1059 | 260 | 2600 | 75 | [116] |

^aResults obtained with two gain media in the resonator. ^bData not given in the corresponding publication

a high gain per length, i.e., operating the disk at a high inversion level. For many materials, the gain bandwidth Δf_g depends strongly on the inversion level (see Fig. 4), which can additionally increase the minimum achievable pulse duration in the thin disk configuration.

As an example, let us compare the results obtained with Yb:YAG. Its gain bandwidth decreases for high inversion levels: for low level excitation, the gain spectrum is substantially broader with a peak at longer wavelengths (Fig. 4). The low power mode-locked laser in Ref. [9] used a 3.5-mm long 5 at.% Yb-doped YAG crystal. A standing-wave cavity is used, which leads to 7 mm total gain length per cavity roundtrip. Pulses as short as 340 fs were achieved at a center wavelength of 1033 nm. The output power of 110 mW was generated with 2% output coupling. In contrast, the high-power Yb:YAG thin disk laser presented in [4, 5] used an output coupling of 8.5%. It generated 80 W of average power in 705-fs pulses. The laser has a substantially shorter propagation length in the gain medium. The 100- μ m disk was 10 at.% Yb-doped and used as a folding mirror, leading to a total gain length of 400 μ m per cavity roundtrip. The emission wavelength was 1030 nm, which is 3 nm shorter than for the low power laser. Both effects, the higher saturated gain and the reduced gain bandwidth due to a high inversion level, increased the minimum achievable pulse duration. Please note that for a more precise discussion on the minimum achievable pulse duration, it is important to consider other effects such as spatial hole burning and to investigate the stability limits numerically. A detailed analysis and discussion of pulse formation in ultrafast thin disk lasers is given in Ref. [8].

There are two main directions for achieving shorter pulse duration. Most importantly, the gain bandwidth has to be increased by choosing a better material with larger emission bandwidth. Another possibility is to reduce the saturated gain, which requires operating the laser at low intracavity losses and low output coupling. Especially for higher pulse energies, this may require to eliminate the nonlinearity resulting from the air in the resonator, e.g., by operating the laser in a helium atmosphere or vacuum. In this way, we prevent excessive self-phase modulation, which would otherwise destabilize the pulse formation [45]. The gain per cavity roundtrip can be increased by using a cavity setup with multiple passes through the gain medium. Such resonators were previously used for pulse energy scaling with a resonator in ambient atmosphere because the high saturated gain enables large output coupling, which substantially reduces intracavity SPM [46]. The laser resonator presented in [7] uses 52 passes through a 60- μ m thick disk, which leads to a total gain length of 3.1 mm per cavity roundtrip. However, with an output coupling of 78%, it was also operated at high saturated gain and high inversion levels, resulting in 928-fs long pulses. Nevertheless, such multiple-pass cavities

are promising for shortening the pulse duration of ultrafast thin disk lasers by enlarging the total gain length per cavity roundtrip. For efficient operation at lower saturated gain, the output coupling and intracavity losses have to be kept sufficiently low. For the above mentioned case, this would require reducing the Kerr nonlinearity of the atmosphere inside the resonator. However, even at very low inversion levels, Yb:YAG does not appear suitable for the generation of sub-100-fs pulses, and alternative gain materials are needed.

4.2 Gain materials with larger emission bandwidth

Ti:sapphire gain material has a particularly high optical gain bandwidth supporting less than 6-fs pulse duration from low energy oscillators [47, 48], which is shorter than for any other laser materials. Unfortunately, its pump wavelength is in the blue-green spectral region, which requires complex and expensive pump lasers. The first CW lasing results with diode pumping were presented very recently, but the obtained output powers were only 8 mW [49]. The development of high-power diode bars operating in the blue-green spectral region is challenging and high-power diode pumping cannot be envisaged in the near future. Furthermore, the material is not well-suited for high-power laser operation at room temperature. The large difference between the emission wavelength and the pump wavelength results in a quantum defect of >30%, which leads to a large amount of deposited heat. The short lifetime results in a high pump threshold, which further increases the heat load in the crystal. So far high doping concentration has not been demonstrated and for the current typical doping concentrations (0.25 at.%) the disk thickness would need to be relatively large even for a 32 pump pass configuration. Therefore, thermal lensing and aberrations would be a challenge even in the thin disk configuration. In summary, Ti:sapphire is not a well-suited material for power scaling in the thin disk approach.

Rare-earth-doped phosphate or silicate glasses also exhibit a very broad emission bandwidth, which supports the generation of pulses with durations of less than 60 fs [50]. Unfortunately, these materials have poor thermal conductivity, which makes them unsuitable for high-power thin disk lasers.

So far, all high-power thin disk lasers used rare-earth-doped crystalline materials such as: garnets (YAG [28], LuAG [51]), sesquioxides (Sc_2O_3 [52], Lu_2O_3 [20], LuScO_3 [19]), tungstates (KYW [52], KGW [52], KLuW [53], NGW [54]), vanadates (LuVO [55], YVO [55], GdVO [56]), and borates (YCOB [57], LSB [58]). The doping ions were Yb^{3+} [28], Nd^{3+} [59], Ho^{3+} [60], and Tm^{3+} [61]. In high-power operation, disk diameters of several millimeters up to centimeters are necessary. This requires a growth method that can provide crystals of this diameter in high

optical quality, such as the Czochralski method [62] or the heat exchanger method (HEM) [63]. Ceramic laser materials might be an interesting alternative [64], but at this time superior performance has not yet been proved in the thin disk approach. Furthermore, until recently, only cubic lattices could be produced as ceramics. The first anisotropic ceramics still suffer from low optical quality [65]. Many interesting laser materials grow in an anisotropic crystal structure. This has the advantage of a linearly polarized laser output but at the expense of anisotropy of the thermomechanical properties which increases the tendency for stress fracture in the disk. However, linear polarization in cubic crystals can be easily obtained by several means, for example, by using an intracavity fused quartz plate introduced at Brewster's angle or a thin-film polarizer.

The most successful laser materials for femtosecond pulse generation and direct diode pumping use the rare-earth-ion ytterbium as a dopant. The simple energy level scheme of the Yb^{3+} -ion makes it very attractive for thin disk lasers. The existence of only two Stark manifolds eliminates the occurrence of parasitic processes even at high doping concentrations and the resulting quasi-three-level character leads to a low quantum defect for the laser operation and hence a low thermal load on the active medium. The peak emission cross section is usually in the spectral range of 1030 to 1060 nm, and the zero-phonon-line (ZPL) absorption around 975 nm. The Yb-ion is very suitable for short pulse generation: a relatively strong coupling of the optical $4f-4f$ -transitions to the phonons of the host leads to broadened absorption and emission spectra which are sufficient for the generation of sub-100-fs pulses in many host materials.

Only in some cases like Yb:YAG, the 940-nm absorption is higher than the ZPL absorption. Today, high-power pump diodes are available for both wavelength ranges. For some materials, the ZPL absorption peak is narrower than the usual emission bandwidth of high-power diodes (3–5 nm). However, during the last years diodes with sufficiently small emission bandwidth have become commercially available. Today power levels of several hundred watts are achieved at <0.5 nm bandwidth from VBG-stabilized laser diodes.

In general, the most suitable hosts for high-power Yb-doped lasers are those where the Yb-ion substitutes Lu. Due to the low mass difference between these ions, the propagation of the phonons, which are mainly responsible for the heat transport in insulators like oxide crystals, is only slightly disturbed. This leads to the lowest decrease in thermal conductivity by the dopant compared to any other ion, including other rare earth sites such as Gd and Y.

The lattice structure also has a strong influence on the thermal material properties. In a disordered lattice different ions are statistically distributed on the same site. This disturbs the propagation of phonons and reduces the thermal

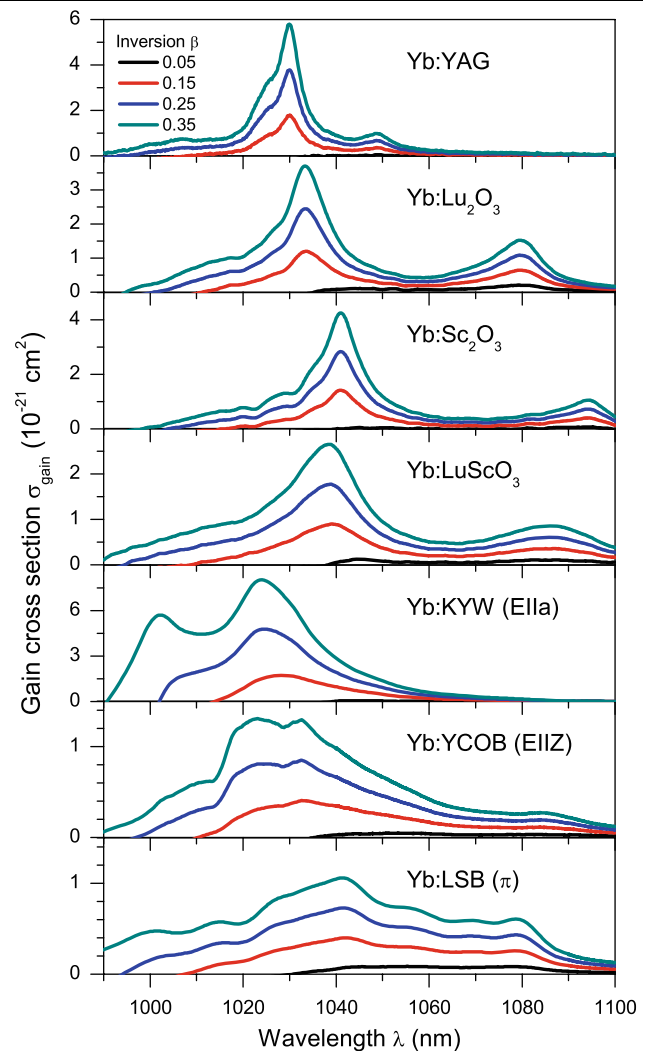


Fig. 4 Gain spectra of the discussed gain materials shown for four different inversion levels β (0.05, 0.15, 0.25, and 0.3, numbers correspond to the total population of the upper laser manifold). For anisotropic materials, the shown spectra correspond to the orientation of maximum gain

conductivity. On the other hand, disordered hosts often exhibit very broad and smooth spectra due to the different lattice environments for the laser active ion.

5 Yb-doped gain materials for ultrafast thin disk lasers

In the following section, we discuss a number of attractive Yb hosts for ultrafast thin disk lasers. In Fig. 4, we show gain spectra at different inversion levels β (calculated as $\sigma_{\text{gain}} = \beta \cdot \sigma_{\text{em}} - (1 - \beta) \cdot \sigma_{\text{abs}}$) for seven Yb-doped materials. The gain spectra were calculated from emission and absorption spectra measured at the ILP Hamburg. Details on these measurements can be found in Refs. [66, 67].

5.1 Yb:garnets

As discussed previously in the text, Yb:YAG is well suited for high-power thin disk lasers, but has a relatively small emission bandwidth among the Yb-doped laser materials. This is a general tendency of all garnet hosts. In the CW-regime Yb:LuAG could be a promising alternative to Yb:YAG because of its better thermal conductivity at high Yb-doping levels. However, it is not promising for generating shorter pulses because its gain bandwidth is even smaller [51].

5.2 Yb:sesquioxides

Another interesting group of gain materials for thin disk lasers are Yb-doped sesquioxides (RE_2O_3 with $\text{RE} = \text{Y}, \text{Sc},$ or Lu). They were among the first materials to be tested as an alternative to Yb:YAG in the thin disk laser geometry [52]. This is due to their lower quantum defect and good thermomechanical properties. They have high thermal conductivity, excellent mechanical stability and a cubic crystal structure. However, for these initial experiments the efficiency proved to be significantly lower compared to Yb:YAG. This was mainly caused by the insufficient crystal quality of the available samples: the high melting point of more than 2400°C is a big challenge for crystal growth. Furthermore, the laser was not pumped at the absorption maximum of 975 nm, but with 940-nm pump diodes.

Recently, the growth process of these materials by the heat exchanger method was optimized, which resulted in Yb-doped sesquioxide crystals of unprecedented optical quality [68]. Furthermore, high-power laser diodes with sufficiently reduced emission bandwidth (<3 nm) became available at 975 nm. This progress made Yb-doped sesquioxides the most efficient thin disk laser materials available nowadays. Optical-to-optical efficiencies well above 70% can be easily achieved in multimode CW operation. Among the different sesquioxides Lu_2O_3 is the most suitable host because it shows the highest thermal conductivity when doped with Yb-ions. For CW operation the output power has recently been scaled up to 149 W [69].

All Yb:sesquioxides exhibit a larger emission bandwidth than Yb:YAG and are therefore more suitable for the generation of ultrashort laser pulses. The first mode-locked Yb: Lu_2O_3 thin disk laser generated 523-fs pulses with an average output power of 24 W [21] at 43% optical-to-optical efficiency, which is higher than for any other mode-locked thin disk laser. Very recently, power-scaling to 63 W in 535-fs-pulses and 40 W in 329-fs pulses was demonstrated [69, 70]. Yb: Sc_2O_3 has not yet been tested in a mode-locked thin disk laser, but we would expect longer pulses than for Yb: Lu_2O_3 due to a slightly narrower emission bandwidth.

Yb: Sc_2O_3 has the potential for slightly higher optical-to-optical efficiencies because of its larger emission cross section. However, it might not be as suitable as Lu_2O_3 for further power scaling because of its lower thermal conductivity when doped with Yb [71].

A considerably larger emission bandwidth can be achieved by combining the 7 nm-shifted emission bands of Yb: Lu_2O_3 and Yb: Sc_2O_3 in the mixed sesquioxide Yb: LuScO_3 [19]. The resulting material exhibits a more than twice as large emission bandwidth. In initial experiments with this material, pulses as short as 227 fs were obtained, which are the shortest pulses from a thin disk laser [22]. The output power of 7.2 W was limited by growth defects of the only available disk and should be considerably increased with disks of better quality. However, the disordered lattice causes a lower thermal conductivity compared to the pure sesquioxides, which makes it hard to compete with the power scaling potential of Yb: Lu_2O_3 , for example.

5.3 Yb:tungstates

The Yb-doped double tungstates $\text{ARE}(\text{WO}_4)_2$ with an alkali-ion A and a rare-earth ion $\text{RE} = \text{Gd}, \text{Lu},$ and Y are very interesting hosts for the thin disk laser. The monoclinic tungstates with K as the alkali ion are of particular interest due to their extremely large cross sections [72]. These crystals are among the most efficient Yb-doped laser materials [73]. Another interesting group is represented by the tetragonal tungstates with Na as the alkali ion, as this group crystallizes in a disordered lattice structure, leading to extremely broad spectra. Yb:NYW (Yb: $\text{NaY}(\text{WO}_4)_2$) and Yb:NGW (Yb: $\text{NGd}(\text{WO}_4)_2$) are among the Yb-doped materials that delivered the shortest pulses (see Table 2).

A disadvantage of tungstates is that most of them cannot be grown by the Czochralski method due to an incongruent melting behavior. Thus, the flux method has to be used [23], which is a technique with very slow growth rates. Consequently, large crystals of high optical quality are harder to obtain than with the Czochralski or heat exchanger method. Additionally, all of these materials crystallize in a non-cubic structure with a strong anisotropy of the thermomechanical properties, which is disadvantageous for high-power lasers.

One of the few materials of this class that can be grown by the Czochralski method is Yb:NGW (Yb: $\text{NaGd}(\text{WO}_4)_2$). However, its low thermal conductivity of only 1.1 W/(m K) resulting from the disordered lattice is comparable to that of glasses and not well suited for high-power thin disk lasers. This was experimentally confirmed with a CW multimode thin disk laser for which the output power was restricted to less than 20 W with an optical-to-optical efficiency of 42% [54].

Yb:KYW (Yb: $\text{KY}(\text{WO}_4)_2$) has been intensively examined for its suitability for the thin disk laser. In CW operation

the output power has been scaled to 73 W at 60% optical-to-optical efficiency [52]. Already in 2002, a thin disk laser based on the Yb:KYW gain material was mode-locked. The laser generated 22 W average output power in 240 fs pulses [18]. Despite these promising initial results, power scaling with this gain material has not yet been demonstrated. Unfortunately, it is difficult to manufacture high-quality thin disks because the host material KYW shows strongly anisotropic thermo-optical and mechanical properties. This challenges stable fundamental mode operation at high pump powers [74, 75].

Yb:KLuW and Yb:KGW exhibit very similar properties compared to those of Yb:KYW. Thin disk laser operation has been demonstrated with both of them [52]. Recently, 440-fs pulses have been realized with an average output power exceeding 25 W with Yb:KLuW. Furthermore, chirped-pulse operation of a thin disk laser oscillator was investigated for the first time with this material [53].

5.4 Yb:vanadates

As can be seen in Table 2, Yb-doped vanadate crystals also enabled the generation of very short femtosecond pulses [76, 77]. Some of these materials such as Yb:LuVO and Yb:YVO have been used in a CW thin disk laser but the output power has not exceeded 15 W [55]. Despite their comparably high thermal conductivity [78] both materials suffer from a very small splitting of the lower Stark level, which makes the laser performance very sensitive to thermal issues. Therefore, these crystals appear not well-suited for the generation of femtosecond pulses in high-power thin disk lasers.

5.5 Yb:borates

Many Yb-doped borates exhibit a disordered crystal structure that can lead to broad spectra. Among the different borates, Yb:YCOB and Yb:LSB have the advantage of a nearly congruent melting behavior, which enables Czochralski growth [79, 80]. Both materials support the generation of sub-100-fs pulses in the low power SESAM-mode-locked regime (see Table 2). They have quite low absorption coefficients compared to the other mentioned thin disk laser materials. Therefore, rather thick disks exceeding 0.5 mm were used in CW thin disk lasers. Despite this fact, output powers exceeding 25 W were realized without any thermal roll-over (LSB: 40 W, YCOB: 26 W) [57, 58]. So far, these promising materials have not been used in ultrafast thin disk lasers, but mode-locked operation with sub-200-fs pulses and several tens of watts average power appears feasible.

6 Conclusion

Ultrafast SESAM-mode-locked thin disk lasers offer a robust and power-scalable solution to the challenges of gener-

ating femtosecond pulses at high power levels without external amplification. The efficient heat removal in the thin disk laser geometry minimizes thermal lensing and aberrations. This enables high power levels in a fundamental transverse mode even for gain materials with relatively low thermal conductivity as is often the case for disordered gain materials with a broad emission bandwidth. Due to its design flexibility, the SESAM is an ideal device for mode locking at such high power levels and pulse energies. The concept of the SESAM-mode-locked thin disk laser has the essential advantage of power scalability: the output power can be scaled up by increasing pump power and mode areas on both gain medium and SESAM by the same factor. The properties of the employed gain material play a crucial role because they determine both the minimum obtainable pulse duration and the achievable output power levels.

Today the highest output powers and pulse energies are still obtained with the garnet Yb:YAG, which was the first thin disk gain material. But with the advances in research and development of new Yb-doped hosts and the availability of suitable pump diodes operating in the 980-nm spectral region, other gain materials have the potential to outperform Yb:YAG in the area of ultrafast pulse generation. However, finding a suitable gain material is not trivial: an ideal femtosecond thin disk gain material has to excel not only in terms of laser properties but also in terms of other material characteristics. In this paper, we discussed gain material requirements and reviewed the most promising candidates. Yb³⁺-doped gain materials have proven to be well suited for thin disk lasers thanks to their low quantum defect and broad amplification bandwidths allowing femtosecond pulse generation. Many crystalline oxide host materials provide thermomechanical properties that are well suited for high-power laser systems.

We expect that femtosecond pulses with several hundred watts of average power will be achieved in the near future. Besides the well-established Yb:YAG gain medium, the sesquioxide Yb:Lu₂O₃ is a promising material for this task. It has already proven its high suitability for the thin disk approach achieving the highest optical-to-optical efficiency of any thin disk laser both in CW multimode (i.e., 73%) and mode-locked operation (i.e., 43%).

Currently, the shortest pulses obtained from an ultrafast thin disk laser are 227 fs achieved with Yb:LuScO₃, another sesquioxide. Other Yb hosts with broader emission spectra appear even more promising to further reduce the pulse duration. Borates such as Yb:LSB and Yb:YCOB are particularly promising. Operation at several tens of watts in the CW regime has been demonstrated, but no mode locking has been demonstrated so far in a thin disk laser. Recently, other established femtosecond laser materials such as Yb:CALGO or different Yb:silicates (see Table 2) also appear promising to extend the performance of ultrafast thin disk lasers into the sub-100-fs regime.

Acknowledgements We would like to acknowledge financial support by the Swiss National Science Foundation (SNSF).

Open Access This article is distributed under the terms of the Creative Commons Attribution Noncommercial License which permits any noncommercial use, distribution, and reproduction in any medium, provided the original author(s) and source are credited.

References

1. J. Aus der Au, G.J. Spühler, T. Südmeyer, R. Paschotta, R. Hövel, M. Moser, S. Erhard, M. Karszewski, A. Giesen, U. Keller, *Opt. Lett.* **25**, 859 (2000)
2. U. Keller, *Nature* **424**, 831 (2003)
3. T. Südmeyer, S.V. Marchese, S. Hashimoto, C.R.E. Baer, G. Gin-gras, B. Witzel, U. Keller, *Nat. Photonics* **2**, 599 (2008)
4. F. Brunner, E. Innerhofer, S.V. Marchese, T. Südmeyer, R. Paschotta, T. Usami, H. Ito, S. Kurimura, K. Kitamura, G. Ar-isholm, U. Keller, *Opt. Lett.* **29**, 1921 (2004)
5. E. Innerhofer, T. Südmeyer, F. Brunner, R. Häring, A. Aschwan-den, R. Paschotta, U. Keller, C. Hönninger, M. Kumkar, *Opt. Lett.* **28**, 367 (2003)
6. S.V. Marchese, C.R.E. Baer, A.G. Engqvist, S. Hashimoto, D.J.H.C. Maas, M. Golling, T. Südmeyer, U. Keller, *Opt. Ex-press* **16**, 6397 (2008)
7. J. Neuhaus, D. Bauer, J. Zhang, A. Killi, J. Kleinbauer, M. Kumkar, S. Weiler, M. Guina, D.H. Sutter, T. Dekorsy, *Opt. Ex-press* **16**, 20530 (2008)
8. R. Paschotta, J. Aus der Au, G.J. Spühler, S. Erhard, A. Giesen, U. Keller, *Appl. Phys. B* **72**, 267 (2001)
9. C. Hönninger, R. Paschotta, M. Graf, F. Morier-Genoud, G. Zhang, M. Moser, S. Biswal, J. Nees, A. Braun, G.A. Mourou, I. Johannsen, A. Giesen, W. Seeber, U. Keller, *Appl. Phys. B* **69**, 3 (1999)
10. F. Brunner, R. Paschotta, J. Aus der Au, G.J. Spühler, F. Morier-Genoud, R. Hövel, M. Moser, S. Erhard, M. Karszewski, A. Giesen, U. Keller, *Opt. Lett.* **26**, 379 (2001)
11. M. Ferray, A. L'Huillier, X.F. Li, L.A. Lompré, G. Mainfray, C. Manus, *J. Phys. B, At. Mol. Opt. Phys.* **21**, L31 (1988)
12. A. McPherson, G. Gibson, H. Jara, U. Johann, T.S. Luk, I.A. McIntyre, K. Boyer, C.K. Rhodes, *J. Opt. Soc. Am. B* **4**, 595 (1987)
13. E. Innerhofer, F. Brunner, S.V. Marchese, R. Paschotta, U. Keller, K. Furusawa, J.C. Baggett, T.M. Monro, D.J. Richardson, in *Ad-vanced Solid-State Photonics (ASSP)*, 2005, paper TuA3
14. T. Südmeyer, F. Brunner, E. Innerhofer, R. Paschotta, K. Furu-sawa, J.C. Baggett, T.M. Monro, D.J. Richardson, U. Keller, *Opt. Lett.* **28**, 1951 (2003)
15. U. Keller, in *Landolt-Börnstein. Laser Physics and Applications. Subvolume B: Laser Systems. Part I*, ed. by G. Herziger, H. We-ber, R. Proprawe (Springer, Heidelberg, 2007), p. 33
16. F. Druon, F. Balembois, P. Georges, *Ann. Chim. Sci. Mat* **28**, 47 (2003)
17. M. Tokurakawa, A. Shirakawa, K. Ueda, H. Yagi, M. Noriyuki, T. Yanagitani, A.A. Kaminskii, *Opt. Express* **17**, 3353 (2009)
18. F. Brunner, T. Südmeyer, E. Innerhofer, R. Paschotta, F. Morier-Genoud, J. Gao, K. Contag, A. Giesen, V.E. Kisel, V.G. Shcher-bitsky, N.V. Kuleshov, U. Keller, *Opt. Lett.* **27**, 1162 (2002)
19. R. Peters, K. Petermann, G. Huber, in *Advanced Solid-State Pho-tonics (ASSP)*, 2009, paper MC4
20. R. Peters, C. Kränkel, K. Petermann, G. Huber, *Opt. Express* **15**, 7075 (2007)
21. S.V. Marchese, C.R.E. Baer, R. Peters, C. Kränkel, A.G. En-gqvist, M. Golling, D.J.H.C. Maas, K. Petermann, T. Südmeyer, G. Huber, U. Keller, *Opt. Express* **15**, 16966 (2007)
22. C.R.E. Baer, C. Kränkel, O.H. Heckl, M. Golling, T. Südmeyer, R. Peters, K. Petermann, G. Huber, U. Keller, *Opt. Express* **17**, 10725 (2009)
23. C. Cascales, M.D. Serrano, F. Esteban-Betegón, C. Zaldo, R. Pe-ters, K. Petermann, G. Huber, L. Ackermann, D. Rytz, C. Dupré, M. Rico, J. Liu, U. Griebner, V. Petrov, *Phys. Rev. B* **74**, 174114 (2006)
24. Y. Jeong, J.K. Sahu, D.N. Payne, J. Nilsson, *Opt. Express* **12**, 6088 (2004)
25. F. Röser, J. Rothhard, B. Ortac, A. Liem, O. Schmidt, T. Schreiber, J. Limpert, A. Tünnermann, *Opt. Lett.* **30**, 2754 (2005)
26. F. Röser, D. Schimpf, O. Schmidt, B. Ortac, K. Rademaker, J. Limpert, A. Tünnermann, *Opt. Lett.* **32**, 2230 (2007)
27. L. Shah, M.E. Fermann, J.W. Dawson, C.P.J. Barty, *Opt. Express* **14**, 12546 (2006)
28. A. Giesen, H. Hügel, A. Voss, K. Wittig, U. Brauch, H. Opower, *Appl. Phys. B* **58**, 365 (1994)
29. A. Giesen, J. Speiser, *IEEE J. Sel. Top. Quantum Electron.* **13**, 598 (2007)
30. J. Mende, J. Speiser, G. Spindler, W.L. Bohn, A. Giesen, in *Solid State Lasers XVII: Technology and Devices*, Proceedings of the SPIE, vol. 6871, ed. by W.A. Clarkson, N. Hodgson, R.K. Shori (2008), p. 68710
31. U. Keller, D.A.B. Miller, G.D. Boyd, T.H. Chiu, J.F. Ferguson, M.T. Asom, *Opt. Lett.* **17**, 505 (1992)
32. U. Keller, K.J. Weingarten, F.X. Kärtner, D. Kopf, B. Braun, I.D. Jung, R. Fluck, C. Hönninger, N. Matuschek, J. Aus der Au, *IEEE J. Sel. Top. Quantum Electron.* **2**, 435 (1996)
33. G.J. Spühler, K.J. Weingarten, R. Grange, L. Krainer, M. Haiml, V. Liverini, M. Golling, S. Schon, U. Keller, *Appl. Phys. B* **81**, 27 (2005)
34. L.R. Brovelli, U. Keller, T.H. Chiu, *J. Opt. Soc. Am. B* **12**, 311 (1995)
35. C. Hönninger, R. Paschotta, F. Morier-Genoud, M. Moser, U. Keller, *J. Opt. Soc. Am. B* **16**, 46 (1999)
36. D.J.H.C. Maas, B. Rudin, A.-R. Bellancourt, D. Iwaniuk, S.V. Marchese, T. Südmeyer, U. Keller, *Opt. Express* **16**, 7571 (2008)
37. M. Haiml, R. Grange, U. Keller, *Appl. Phys. B* **79**, 331 (2004)
38. F.X. Kärtner, U. Keller, *Opt. Lett.* **20**, 16 (1995)
39. I.D. Jung, F.X. Kärtner, L.R. Brovelli, M. Kamp, U. Keller, *Opt. Lett.* **20**, 1892 (1995)
40. F.X. Kärtner, I.D. Jung, U. Keller, *IEEE J. Sel. Top. Quantum Electron.* **2**, 540 (1996)
41. R. Paschotta, U. Keller, *Appl. Phys. B* **73**, 653 (2001)
42. G. Palmer, M. Emons, M. Siegel, A. Steinmann, M. Schultze, M. Lederer, U. Morgner, *Opt. Express* **15**, 16017 (2007)
43. O.M. Efimov, L.B. Glebov, L.N. Glebova, K.C. Richardson, V.I. Smirnov, *Appl. Opt.* **38**, 619 (1999)
44. G.B. Venus, A. Sevan, V.I. Smirnov, L.B. Glebov, in *Confer-ence on High-Power Diode Laser Technology and Applications III*, 2005, p. 166
45. S.V. Marchese, T. Südmeyer, M. Golling, R. Grange, U. Keller, *Opt. Lett.* **31**, 2728 (2006)
46. J. Neuhaus, J. Kleinbauer, A. Killi, S. Weiler, D. Sutter, T. Deko-rsy, *Opt. Lett.* **33**, 726 (2008)
47. D.H. Sutter, G. Steinmeyer, L. Gallmann, N. Matuschek, F. Morier-Genoud, U. Keller, V. Scheuer, G. Angelow, T. Tschudi, *Opt. Lett.* **24**, 631 (1999)
48. U. Morgner, F.X. Kärtner, S.H. Cho, Y. Chen, H.A. Haus, J.G. Fujimoto, E.P. Ippen, V. Scheuer, G. Angelow, T. Tschudi, *Opt. Lett.* **24**, 411 (1999)
49. A.J. Maclean, P. Roth, G.J. Valentine, A.J. Kemp, D. Burns, in *Advanced Solid-State Photonics (ASSP)*, 2009, paper WE2
50. C. Hönninger, F. Morier-Genoud, M. Moser, U. Keller, L.R. Brovelli, C. Harder, *Opt. Lett.* **23**, 126 (1998)

51. K. Beil, S.T. Friedrich-Thornton, R. Peters, K. Petermann, G. Huber, in *Advanced Solid-State Photonics (ASSP)*, 2009, paper WB28
52. M. Larionov, J. Gao, S. Erhard, A. Giesen, K. Contag, V. Peters, E. Mix, L. Fornasiero, K. Petermann, G. Huber, J. Aus der Au, G.J. Spühler, R. Paschotta, U. Keller, A.A. Lagatsky, A. Abdolvand, N.V. Kuleshov, in *Advanced Solid-State Lasers (OSA, 2001)*, p. 625
53. G. Palmer, M. Schultze, M. Siegel, M. Emons, U. Bunting, U. Morgner, *Opt. Lett.* **33**, 1608 (2008)
54. R. Peters, C. Kränkel, K. Petermann, G. Huber, *Appl. Phys. B* **91**, 25 (2008)
55. C. Kränkel, R. Peters, K. Petermann, G. Huber, in *Advanced Solid-State Photonics (ASSP)*, 2007, paper MA 3
56. N. Pavel, C. Kränkel, R. Peters, K. Petermann, G. Huber, *Appl. Phys. B* **91**, 415 (2008)
57. C. Kränkel, R. Peters, K. Petermann, P. Loiseau, G. Aka, G. Huber, *J. Opt. Soc. Am. B* **26**, 1310 (2009)
58. C. Kränkel, J. Johannsen, R. Peters, K. Petermann, G. Huber, *Appl. Phys. B* **87**, 217 (2007)
59. A. Giesen, G. Hollemann, I. Johannsen, in *Conference on Lasers and Electro-Optics* (Optical Society of America, Washington, 1999), p. 29
60. M. Schellhorn, *Appl. Phys. B* **85**, 549 (2006)
61. N. Berner, A. Diening, E. Heumann, G. Huber, A. Voss, M. Karszewski, A. Giesen, in *Topical Meeting on Advanced Solid-State Lasers* (Optical Society of America, Washington, 1999), p. 463
62. J. Czochralski, *Z. Phys. Chem. Stoechiom. Verwandtschafts* **92**, 219 (1917)
63. F. Schmid, *D. Viechnic, J. Am. Ceram. Soc.* **53**, 528 (1970)
64. M. Tokurakawa, A. Shirakawa, K. Ueda, H. Yagi, S. Hosokawa, T. Yanagitani, A.A. Kaminskii, *Opt. Lett.* **33**, 1380 (2008)
65. J. Akiyama, Y. Sato, T. Taira, in *Advanced Solid-State Photonics (ASSP)*, 2009, paper PD MF1
66. C. Kränkel, PhD Thesis, University of Hamburg, Germany, 2008
67. R. Peters, PhD Thesis, University of Hamburg, Germany, 2009
68. R. Peters, C. Kränkel, K. Petermann, G. Huber, *J. Cryst. Growth* **310**, 1934 (2008)
69. C.R.E. Baer, C. Kränkel, C.J. Saraceno, O.H. Heckl, M. Golling, T. Südmeyer, R. Peters, K. Petermann, G. Huber, U. Keller, in *Conference on Lasers and Electro-Optics (Europe)*, 2009, paper CA2.3
70. C.R.E. Baer, C. Kränkel, C.J. Saraceno, O.H. Heckl, M. Golling, T. Südmeyer, R. Peters, K. Petermann, G. Huber, U. Keller, *Opt. Lett.* (2009). http://www.opticsinfobase.org/DirectPDFAccess/4B5F7A60-BDB9-137ECD902F636B82DA80_112117.pdf?da=1&id=112117&seq=0&CFID=37778031&CFTOKEN=36341418
71. R. Peters, C. Kränkel, K. Petermann, G. Huber, in *Conference on Lasers and Electro-Optics*, 2008, paper CTuKK4
72. V. Petrov, M.C. Pujol, X. Mateos, O. Silvestre, S. Rivier, M. Aguilo, R.M. Sole, J.H. Liu, U. Griebner, F. Diaz, *Laser Photon. Rev.* **1**, 179 (2007)
73. N.V. Kuleshov, A.A. Lagatsky, A.V. Podlipensky, V.P. Mikhailov, G. Huber, *Opt. Lett.* **22**, 1317 (1997)
74. A.A. Kaminskii, A.F. Konstantinova, V.P. Orekhova, A.V. Butashin, R.F. Klevtsova, A.A. Pavlyuk, *Crystallogr. Rep.* **46**, 665 (2001)
75. S. Biswal, S.P. O'Connor, S.R. Bowman, *Appl. Opt.* **44**, 3093 (2005)
76. A.A. Lagatsky, A.R. Sarmani, C.T.A. Brown, W. Sibbett, V.E. Kisel, A.G. Selivanov, I.A. Denisov, A.E. Troshin, K.V. Yumashev, N.V. Kuleshov, V.N. Matrosov, T.A. Matrosova, M.I. Kupchenko, *Opt. Lett.* **30**, 3234 (2005)
77. S. Rivier, X. Mateos, J. Liu, V. Petrov, U. Griebner, M. Zorn, M. Weyers, H. Zhang, J. Wang, M. Jiang, *Opt. Express* **14**, 11668 (2006)
78. C. Kränkel, D. Fagundes-Peters, S.T. Friedrich, J. Johannsen, M. Mond, G. Huber, M. Bernhagen, R. Uecker, *Appl. Phys. B* **79**, 543 (2004)
79. Q. Ye, B.H.T. Chai, *J. Cryst. Growth* **197**, 228 (1999)
80. S.A. Kutovoi, V.V. Laptev, S.Y. Matsnev, *Sov. J. Quantum Electron.* **21**, 131 (1991)
81. P.F. Moulton, *J. Opt. Soc. Am. B* **3**, 125 (1986)
82. W. Koechner, *Solid-State Laser Engineering*, 6 edn., Springer Series in Optical Sciences, vol. 1 (Springer Science+Business Media, Inc., New York, 2006)
83. I.H. Malitson, *J. Opt. Soc. Am.* **52**, 1377 (1962)
84. J.J. Zayhowski, J. Harrison, in *Handbook of Photonics*, ed. by M.C. Gupta (CRC Press, New York, 1997), p. 326
85. J.E. Geusic, H.M. Marcos, L.G.V. Uitert, *Appl. Phys. Lett.* **4**, 182 (1964)
86. J.H. Liu, X. Mateos, H.J. Zhang, J. Li, J.Y. Wang, V. Petrov, *IEEE J. Quantum Electron.* **43**, 385 (2007)
87. D. Jaque, J. Capmany, J. Rams, J.G. Sole, *J. Appl. Phys.* **87**, 1042 (2000)
88. J. Petit, P. Goldner, B. Viana, *Opt. Lett.* **30**, 1345 (2005)
89. A.A. Lagatsky, N.V. Kuleshov, V.P. Mikhailov, *Opt. Commun.* **165**, 71 (1999)
90. M. Larionov, K. Schuhmann, J. Speiser, C. Stolzenburg, A. Giesen, in *Advanced Solid-State Photonics (ASSP)*, 2005, paper TuB49
91. S. Dewald, T. Lang, C.D. Schroter, R. Moshhammer, J. Ullrich, M. Siegel, U. Morgner, *Opt. Lett.* **31**, 2072 (2006)
92. S. Naumov, A. Fernandez, R. Graf, P. Dombi, F. Krausz, A. Apolonski, *New J. Phys.* **7**, 216 (2005)
93. U. Morgner, F.X. Kärtner, S.H. Cho, Y. Chen, H.A. Haus, J.G. Fujimoto, E.P. Ippen, V. Scheuer, G. Angelow, T. Tschudi, *Opt. Lett.* **24**, 920 (1999)
94. R. Ell, U. Morgner, F.X. Kärtner, J.G. Fujimoto, E.P. Ippen, V. Scheuer, G. Angelow, T. Tschudi, M.J. Lederer, A. Boiko, B. Luther-Davies, *Opt. Lett.* **26**, 373 (2001)
95. S. Uemura, K. Torizuka, *Appl. Phys. Express* **1**, 3 (2008)
96. J. Aus der Au, S.F. Schaer, R. Paschotta, C. Hönninger, U. Keller, M. Moser, *Opt. Lett.* **24**, 1281 (1999)
97. S. Rivier, U. Griebner, V. Petrov, H. Zhang, J. Li, J. Wang, J. Liu, *Appl. Phys. B* **93**, 753 (2008)
98. Y. Zaouter, J. Didierjean, F. Balembois, G. Lucas Leclin, F. Druon, P. Georges, J. Petit, P. Goldner, B. Viana, *Opt. Lett.* **31**, 119 (2006)
99. D.N. Papadopoulos, F. Druon, J. Boudeile, I. Martial, M. Hanna, P. Georges, P.O. Petit, P. Goldner, B. Viana, *Opt. Lett.* **34**, 196 (2009)
100. A. Lucca, M. Jacquemet, F. Druon, F. Balembois, P. Georges, P. Camy, J.L. Doualan, R. Moncorge, *Opt. Lett.* **29**, 1879 (2004)
101. P. Klopp, V. Petrov, U. Griebner, K. Petermann, R. Peters, G. Erbert, *Opt. Lett.* **29**, 391 (2004)
102. A. Schmidt, X. Mateos, V. Petrov, U. Griebner, R. Peters, K. Petermann, G. Huber, A. Klehr, G. Erbert, in *Advanced Solid-State Photonics (Denver, USA, 2009)*, paper MB12
103. G. Paunescu, J. Hein, R. Sauerbrey, *Appl. Phys. B* **79**, 555 (2004)
104. F. Brunner, G.J. Spühler, J. Aus der Au, L. Krainer, F. Morier-Genoud, R. Paschotta, N. Lichtenstein, S. Weiss, C. Harder, A.A. Lagatsky, A. Abdolvand, N.V. Kuleshov, U. Keller, *Opt. Lett.* **25**, 1119 (2000)
105. G.R. Holtom, *Opt. Lett.* **31**, 2719 (2006)
106. H. Liu, J. Nees, G. Mourou, *Opt. Lett.* **26**, 1723 (2001)
107. A.L. Calendron, K.S. Wentsch, M.J. Lederer, *Opt. Express* **16**, 18838 (2008)

108. U. Griebner, S. Rivier, V. Petrov, M. Zorn, G. Erbert, M. Weyers, X. Mateos, M. Aguilo, J. Massons, F. Diaz, *Opt. Express* **13**, 3465 (2005)
109. S. Rivier, M. Rico, U. Griebner, V. Petrov, M.D. Serrano, F. Esteban-Betegón, C. Cascales, C. Zaldo, M. Zorn, M. Weyers, in *Conference on Lasers and Electro-Optics Europe*, 2005, paper CF-4-THU
110. A. García-Cortés, J.M. Cano-Torres, M.D. Serrano, C. Cascales, C. Zaldo, S. Rivier, X. Mateos, U. Griebner, V. Petrov, *IEEE J. Quantum Electron.* **43**, 758 (2007)
111. H. Luo, D.Y. Tang, G.Q. Xie, H.J. Zhang, L.J. Qin, H.H. Yu, L.Y. Ng, L.J. Qian, *Opt. Commun.* **281**, 5382 (2008)
112. X. Mateos, A. Schmidt, V. Petrov, U. Griebner, H.J. Zhang, J.Y. Wang, J.H. Liu, in *Advanced Solid-State Photonics (ASSP)*, 2009, paper MB9
113. F. Druon, F. Balembois, P. Georges, A. Brun, A. Courjaud, C. Hönniger, F. Salin, A. Aron, F. Mougél, G. Aka, D. Vivien, *Opt. Lett.* **25**, 423 (2000)
114. S. Rivier, A. Schmidt, C. Kränkel, R. Peters, K. Petermann, G. Huber, M. Zorn, M. Weyers, A. Klehr, G. Erbert, V. Petrov, U. Griebner, *Opt. Express* **15**, 15539 (2007)
115. F. Druon, S. Chenais, P. Raybaut, F. Balembois, P. Georges, R. Gaume, G. Aka, B. Viana, S. Mohr, D. Kopf, *Opt. Lett.* **27**, 197 (2002)
116. F. Thibault, D. Pelenc, F. Druon, Y. Zaouter, M. Jacquemet, P. Georges, *Opt. Lett.* **31**, 1555 (2006)
117. F. Druon, F. Balembois, P. Georges, *Opt. Express* **12**, 5005 (2004)